

**Preparation of 8:** A solution of *N*-( $\alpha$ -bromobenzylidene)-*N'*-phenylhydrazine (114 mg, 0.47 mmol) and  $\text{NEt}_3$  (100  $\mu\text{L}$ , 0.70 mmol) in toluene (10 mL) was added to a solution of hexafluoropropene ( $\approx$ 150 mg, 1 mmol) in toluene (10 mL) below  $-50^\circ\text{C}$ , and allowed to react at  $100^\circ\text{C}$  for 3 days in a pressure bottle (125 mL, Ace Glass Inc.). The crude product was purified by column chromatography (silica gel, hexane/benzene (9:1)) to give **8** as a yellow oil. Yield: 42 mg (26 %);  $^1\text{H NMR}$  (300 MHz,  $\text{CDCl}_3$ ):  $\delta$  [ppm] = 7.85 (dd, 2H,  $J$  = 7.6, 2.4 Hz), 7.40–7.49 (m, 7H), 7.32–7.39 (m, 1H);  $^{13}\text{C NMR}$  (75 MHz,  $\text{CDCl}_3$ ):  $\delta$  = 143.88 ppm (td,  $J_{\text{C,F}}$  = 22,  $J_{\text{C,F}}$  = 4 Hz), 138.88, 130.98, 129.08, 129.04, 127.75, 126.20, 126.02 (td,  $J_{\text{C,F}}$  = 2,  $J_{\text{C,F}}$  = 1), 125.15, 123.37 (td,  $J_{\text{C,F}}$  = 266,  $J_{\text{C,F}}$  = 23;  $\text{CF}_2$ ), 119.47 (qd,  $J_{\text{C,F}}$  = 283,  $J_{\text{C,F}}$  = 44;  $\text{CF}_3$ ), 98.50 (m; CF);  $^{19}\text{F NMR}$  (282 MHz,  $\text{CDCl}_3$  as solvent,  $\text{CF}_3\text{COOH}$  as  $^{19}\text{F}$  standard):  $\delta$  [ppm] =  $-148.62$  (3F),  $-117.98$  (2F),  $-77.25$  (1F); HRMS (EI) calcd. (found) for  $\text{C}_{16}\text{H}_{10}\text{F}_6\text{N}_2$ : 344.0748 (344.0724); anal. calcd. (found) for  $\text{C}_{16}\text{H}_{10}\text{F}_6\text{N}_2$ : C 55.82 (55.32), H 2.93 (3.29), N 8.14 (7.90).

Received: October 8, 2001  
Final version: May 28, 2002

- [1] For example: a) K. Yagi, Z. Yoshida, T. Tabata, *Fluorescence*, Nankodo, Tokyo **1958**. b) M. J. Heller, L. E. Morrison, in *Rapid Detection and Identification of Infectious Agents* (Eds: D. T. Kingsbury, S. Falkow), Academic Press, New York **1985**, pp. 245–256. c) C. W. Tang, S. A. van Slyke, *Appl. Phys. Lett.* **1987**, *51*, 913. d) B. M. Krasovitskii, B. M. Bolotin, *Organic Luminescent Materials*, VCH, Weinheim **1989**. e) K. Tamao, M. Uchida, T. Izumigawa, K. Furukawa, S. Yamaguchi, *J. Am. Chem. Soc.* **1996**, *118*, 11 974. f) K. Hatchison, J. Gao, G. Schick, Y. Rubin, F. Wudl, *J. Am. Chem. Soc.* **1999**, *121*, 5611. g) X. Gao, H. Cao, L. Q. Zhang, B. W. Zhang, Y. Cao, C. H. Huang, *J. Mater. Chem.* **1999**, *9*, 1077. h) X. H. Zhang, W. Y. Lai, Z. Q. Gao, T. C. Wong, C. S. Lee, H. L. Kwang, S. T. Lee, S. K. Wa, *Chem. Phys. Lett.* **2000**, *320*, 77.
- [2] R. H. Wiley, C. H. Jarboe, F. N. Hayes, E. Hansbury, J. T. Nielsen, P. X. Callahan, M. C. Sellars, *J. Org. Chem.* **1958**, *23*, 732.
- [3] R. Huisgen, M. Seidel, G. Wallbillich, H. Knapfer, *Tetrahedron* **1962**, *17*, 3.
- [4] **5** was synthesized by applying the synthetic method for **6** [5] because of the difficulty in obtaining the original paper (A. S. Morkovnik, O. Y. Okhlobystin, *Khim. Geterotsikl. Soedin.* **1985**, *4*, 551).
- [5] J. S. Clovis, A. Eckell, R. Huisgen, R. Sustman, G. Wallhillich, V. Weberndörfer, *Chem. Ber.* **1967**, *100*, 1593.
- [6] R. Huisgen, H. Knapfer, R. Sustman, G. Wallbillich, V. Weberndörfer, *Chem. Ber.* **1967**, *100*, 1580.
- [7] Spectroscopic data of **5** and **8** are described in the Experimental section. All other pyrazolines (**3**, **4**, **6**, and **7**) were synthesized according to published procedures ([2], [3], [5], and [6], respectively). Pyrazolines described here were wholly characterized by spectroscopic methods, and purified by repeated column chromatography. The distortionless enhancement by polarization transfer (DEPT) technique was also used for confirmation of the structure of cycloadducts **5**, **6**, and **7**.
- [8] As far as luminescent efficiency and photostability are concerned, perylenediimides have been known as state-of-the-art substances (see, for example, F. O. Holtrup, G. R. J. Müller, H. Quante, S. Defeyer, F. C. De Schryver, K. Müllen, *Chem. Eur. J.* **1997**, *3*, 219). However, our preliminary comparison has indicated **8** to be superior to perylenediimides; details will be reported in due course.

## Generation of Chrome Masks with Micrometer-Scale Features Using Microlens Lithography\*\*

By Hongkai Wu, Teri W. Odom, and George M. Whitesides\*

This paper describes the application of microlens array photolithography (MAP) for the fabrication and rapid prototyping of chrome masks having simple, repetitive patterns with

sub-micrometer features. We have used arrays of microlenses and macroscopic (mm- to cm-sized) transparency films as photomasks to generate periodic patterns with microscopic features in photoresist supported on glass. These patterns in photoresist can have symmetries and periodicities different from that of the lens array; this characteristic makes MAP a convenient technique with which to generate patterned arrays of isolated and connected features.<sup>[1–3]</sup> Deposition of a chromium film, followed by lift-off, converts the photoresist pattern into a chrome mask that can be used in contact photolithography to transfer these patterns into other substrates. The roughness of the edges of the chrome mask produced by MAP is  $\sim$ 100 nm, which is comparable to that of chrome masks made by laser writing.<sup>[4,5]</sup>

Chrome masks are used throughout photolithography. Commercial chrome photomasks are conventionally fabricated using e-beam or laser writing;<sup>[6–8]</sup> either type of process can produce high-quality photomasks with arbitrary patterns. E-beam lithography can generate features with sizes down to 10 nm,<sup>[9–11]</sup> and laser writing down to  $\sim$ 500 nm.<sup>[4,5]</sup> These methods are time-consuming because the pattern is written serially and require expensive and sophisticated facilities. We described an approach to features with sizes down to 15  $\mu\text{m}$  that uses transparency films printed from a high-resolution image setter as photomasks in contact photolithography.<sup>[12–15]</sup> To create patterns of smaller features—0.1 to 10  $\mu\text{m}$ —we developed reduction methods that eliminate the grain-size limitation of the transparency film (15  $\mu\text{m}$ ) and are limited instead to the diffraction of light (a few hundred nanometers).

Reduction lithographic techniques such as microscope projection photolithography (MPP)<sup>[16]</sup> and MAP<sup>[1–3,17,18]</sup> can, using masks made from transparencies, generate patterns having micrometer-sized features. In a single exposure, MPP is limited to patterning small areas ( $\sim$ 100  $\mu\text{m}^2$ ), while MAP can generate features down to sub-micrometer over much larger areas ( $\text{cm}^2$ ). The inexpensive and convenient equipment used in MAP—an overhead projector as an illumination source and transparency films from a desktop printer as photomasks—provides access to  $\text{cm}^2$ -sized areas of micrometer and sub-micrometer features without the expense and delay required to produce commercially available chrome masks. Rapid prototyping of certain types of chrome masks (e.g., those having simple patterns with high periodic regularity) using MAP is useful for researchers without routine access to laser and e-beam writers. Those masks can be used to fabricate microarrays, cell-patterning substrates, optical diffractive gratings, and data storage media.<sup>[19,20]</sup> This technique also enables the generation of masters useful in soft lithography, such as arrays of small prototype devices (e.g., microfluidic networks) and other test patterns.

Figure 1 summarizes the procedure for generating arrays of sub-micrometer patterns in photoresist by MAP (see Experimental). The fabrication of the microlens array assembly has been described in detail elsewhere.<sup>[18]</sup> For this experiment, the assembly was formed in two steps: 1) melting and reflowing photoresist posts (3  $\mu\text{m}$  in diameter and spaced by 4.5  $\mu\text{m}$ ,

[\*] Prof. G. M. Whitesides, Dr. H. Wu, Dr. T. W. Odom  
Department of Chemistry and Chemical Biology, Harvard University  
12 Oxford St., Cambridge, MA 02138 (USA)  
E-mail: gwhitesides@gmwgroup.harvard.edu

[\*\*] This work was supported by DARPA. T.W.O. thanks the NIH for a postdoctoral fellowship.

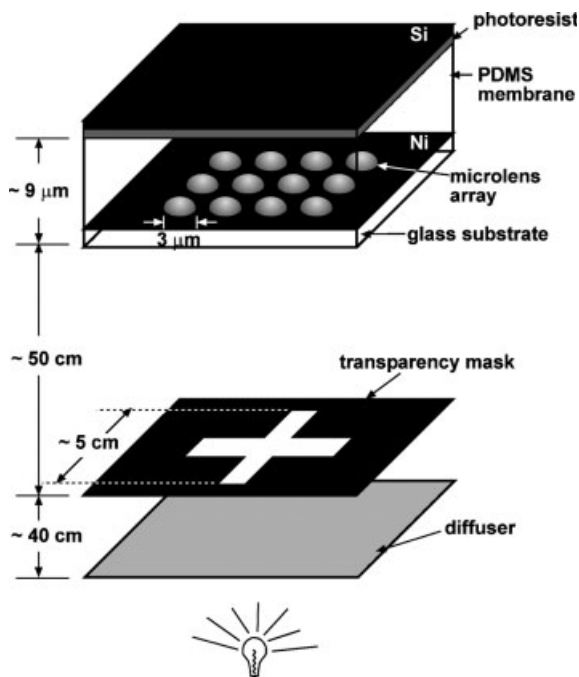


Fig. 1. Schematic illustration of microlens array photolithography. This figure is not to scale and the thickness of the PDMS membrane is exaggerated to show the microlens array. The nickel film (see Experimental) was used to prevent light from leaking from the inter-space between lenses.

Shipley 1805) at a temperature  $T$  ( $120^\circ\text{C}$ )  $>$   $T_g$  (glass transition temperature of the photoresist,  $\sim 105^\circ\text{C}$ ),<sup>[21]</sup> and 2) spinning and curing a thin layer of PDMS, equal to the focal length of the lenses ( $9\ \mu\text{m}$ ), on the top of the microlens array. This lens assembly was situated at a large distance (50 cm) from a transparency mask having cm-sized features and placed in contact with a thin layer of photoresist (400 nm, Shipley 1805) supported on glass. Illumination from an overhead projector passed through the mask and was focused by the lenses; after development, a patterned array of the figure on the mask was produced in the photoresist.

To demonstrate the reduction capabilities of this microlens array (Fig. 2A), we reduced an “X”-shaped figure (20 mm across, 3 mm linewidth) on the photomask into an array of micro-“x”s ( $\sim 2.5\ \mu\text{m}$  across,  $\sim 800\ \text{nm}$  linewidth) in photoresist (Fig. 2B). These “x”s were well separated and exhibited the same symmetry ( $D_{4h}$ ) as the lens array. We also reduced a more complex photomask with the letter “G”, which had curved regions and a sharp corner with an overall larger size (32 mm vs. 20 mm). The two-dimensional (2D) chiral shape of the letter was inverted and reduced by each lens into the photoresist (Fig. 2C). Although rounded at the sharp

corner (probably due to diffraction), the images reproduced the mask at the curved portions well. The size reduction we achieved was  $\sim 10^4$ , and the smallest feature size we obtained from this microlens array was  $500\ \text{nm}$ . Areas as large as  $\sim 1\ \text{cm}^2$  were patterned in photoresist in a single exposure without obvious distortions.<sup>[18]</sup>

Adjacent images in Figure 2C overlapped slightly due to the larger size of the figure on this mask than that used in Figure 2B. We can take advantage of this overlap to create periodic patterns of grids and lines. We have shown recently that the images formed by microlens arrays can connect with each other when the overall size of the figure in a photomask is beyond a critical lateral size  $l_c$  whose value is the product of the spacing of the lenses along high symmetry directions and the overall size reduction.<sup>[2]</sup> In MAP, the distance between the lenses and the mask ( $\sim 50\ \text{cm}$ ) can be seen as infinitely large compared to the focal length of the microlenses ( $9\ \mu\text{m}$ ); thus,  $l_c$  is practically independent of the distance from the lenses to the mask. For these lenses,  $l_c$  was  $\sim 40\ \text{mm}$  along the direction of a microlens to its nearest neighbor. A transparency mask having a cross figure with an overall size (100 mm in both dimensions) much larger than the critical size and oriented with the lens array produced a grid of  $\sim 3.8\ \mu\text{m}$  squares in photoresist spaced by  $\sim 700\ \text{nm}$  (Fig. 3A).

Although the generated patterns usually have the same symmetry, orientation, and pitch as the microlens array, we have demonstrated that the cm-sized transparency masks can be easily changed or simply rotated<sup>[2]</sup> relative to the microlens array to form patterns having a symmetry, orientation, and pitch different from that of the microlens array.

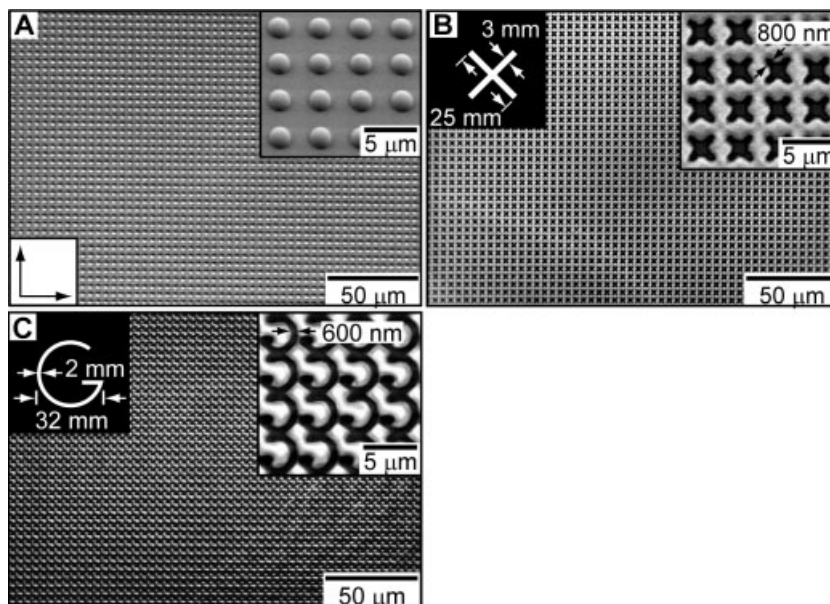


Fig. 2. Scanning electron microscopy (SEM) images of the microlens array and patterned photoresist substrates. A) Array of  $3\ \mu\text{m}$  photoresist lenses. The bottom left inset shows the orientation of the microlens array; the arrows are along the direction from a lens to its nearest neighbors. This same orientation applies to the rest of the Figures. B,C) Photoresist (bright regions) patterns generated on Si (dark regions) wafers using the microlens array shown in (A) with transparency masks (schematically shown as the left top insets) having shapes of an “x” (B) or “G” (C). The right top insets in all images are zoom-in images.

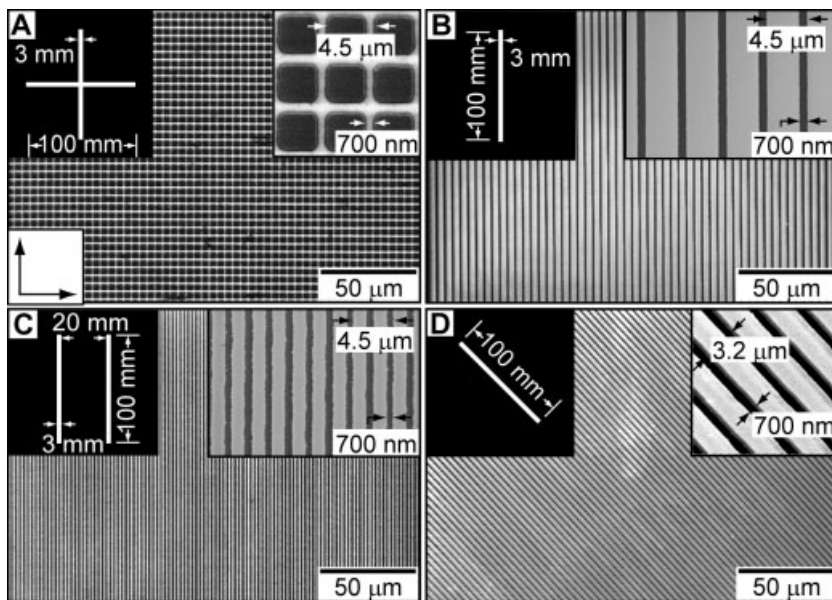


Fig. 3. SEM images of patterns generated in photoresist on Si wafers using the microlens array shown in Figure 2A with masks (schematically shown as the left top insets) having the shape of A) a cross with lateral size of 100 mm, B) a single line and C) two parallel lines having the same orientation as the lens array, and D) a single line having an orientation of  $45^\circ$  relative to the lens array. The left bottom inset in (A) indicates the orientation of the microlens array used in the experiments; the arrows are along the direction from a lens to its nearest neighbors. The right top insets are zoom-in images.

This capability of MAP is desirable for prototyping of chrome masks because the generation of different patterns does not require the fabrication of a new array of microlenses. Figure 3B shows that a photomask having a single, straight line produced cm-long, sub-micrometer parallel lines in photoresist supported on glass. The symmetry ( $D_{2h}$ ) of the line pattern that was formed was lower than that of the microlens array ( $D_{4h}$ ).

In general, there are two approaches that can be used to change the pitch in the patterns generated using MAP: i) repeating the figure on the mask and ii) varying the orientation of the mask figure relative to the microlens array.<sup>[2]</sup> If the masks are designed with  $n$  identical figures separated by a distance of  $1/n \times l_c$  along a dimension, the periodicity in the pattern formed is increased by  $n$ -fold in that dimension. A photomask (Fig. 3C) having two parallel lines ( $n=2$ ) separated by a distance about half of  $l_c$  (20 mm) produced a pattern of parallel lines that had a periodicity that was doubled over that of the pattern shown in Figure 3B. An example of increasing the periodicity by a simple rotation of the mask is shown in Figure 3D. When the line on the mask was aligned along the direction of a lens to its next nearest neighbors, a pattern of parallel lines with a smaller spacing ( $3.2 \mu\text{m}$ ) than that of the microlens array ( $4.5 \mu\text{m}$ ) was formed.

We transferred these patterns of grids and lines in photoresist on glass into chromium (80 nm) with e-beam evaporation and lifted-off the photoresist in acetone to create chrome masks (Figs. 4A,B). The edge roughness<sup>[14,22]</sup> of these masks is between 50–100 nm, which is worse than that of a commercial chrome mask produced by e-beam writing ( $< 30 \text{ nm}$ ),<sup>[9–11]</sup> but comparable to that by laser writing.<sup>[4,5]</sup> We demonstrated their capability in contact photolithography by transferring their pattern to photoresist-coated silicon substrates. We exposed thin ( $\sim 400 \text{ nm}$ ) layers of photoresist (Shipley 1805) to UV-light (365–450 nm) through these masks in a standard mask aligner, developed and removed the exposed photoresist, and obtained patterns in photoresist on silicon wafers (Fig. 4C,D). The patterns on chrome masks were transferred faithfully onto the silicon wafers, and the photoresist patterns on the silicon wafers had the same roughness as that of the chrome masks.

This communication demonstrates that microlens array photolithography provides a convenient route for rapid prototyping of chrome masks with periodic patterns. These masks can have patterned areas  $\sim 1 \times 1 \text{ cm}^2$  and have feature sizes down to 500 nm with an edge roughness of  $\sim 100 \text{ nm}$ . Used in contact photolithography, the patterns on these masks are transferred onto other substrates with high fidelity. Advan-

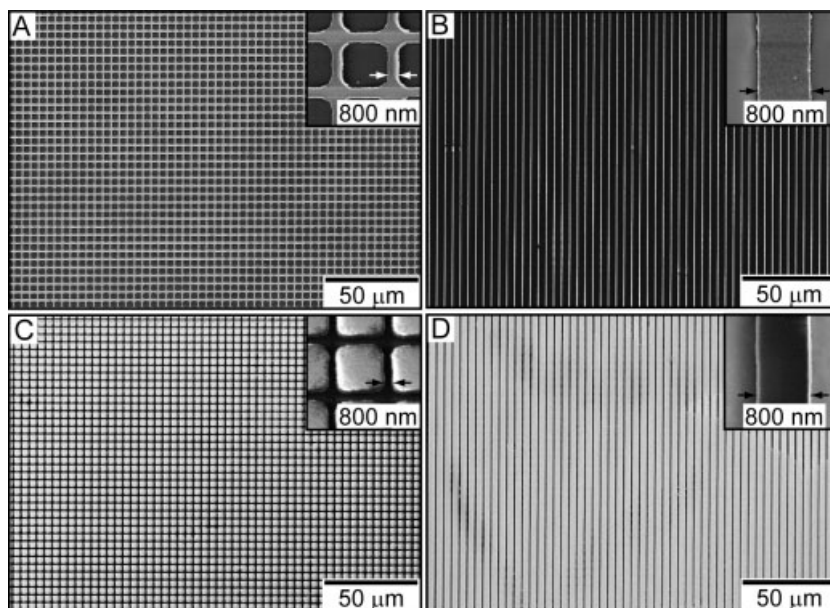


Fig. 4. SEM images of the patterns shown in Figures 3A and 3B formed Cr patterns on glass shown in (A) and (B), respectively. Using these Cr patterns as photomasks in contact photolithography, we generated patterns (C) and (D) of photoresist on a Si wafer, respectively. The insets in all the Figures show zoom-in images.

tages of using MAP for the generation of chrome masks include: i) convenient production of simple patterns with 0.5–10 μm features reduced from cm-sized figures on transparency films; ii) low cost. The expense is effectively equal to the cost to print a transparency film from a desktop printer (< \$1), much less than the cost from e-beam and lasers writing (> \$500); iii) fast turn-around time (production time for a chrome mask by MAP is one day versus one week by e-beam writing); iv) large patterned areas (~1–5 cm<sup>2</sup>) in a single exposure step; and v) long lifetime of a microlens array. A microlens-array assembly can be used many times, as long as it is not broken, with little or no effect on its focusing or reduction capabilities. Disadvantages of using MAP for the fabrication of chrome masks include: i) the patterns are limited to simple, repetitive patterns; ii) the fabrication of the microlens array relies on chrome masks and conventional photolithography; iii) size distortions can occur at the edges of the pattern at areas greater than 1 cm from the center of the lens array, and are expected to be larger than that with conventional chrome masks. This technique for generating chrome masks with periodic patterns is not limited to the array of microlenses here—microlens arrays with other dimensions, lattice spacings and symmetries can generate patterns with many different feature sizes and symmetries.

### Experimental

**Fabrication of Microlens Array:** Glass slides were cleaned by sonicating in acetone and methanol for 5 min. A thin layer of titanium (2 nm) followed by 10 nm of gold was deposited by e-beam evaporation on these slides. We spin-coated a thin layer (~1 μm) of positive photoresist (Shipley 1813, 5000 rpm for 40 s) on these gold-coated slides. This layer of photoresist was exposed through a photomask, patterned with 3 μm circles spaced by 1.5 μm, for 5 s in a Karl Suss mask aligner with a UV-light source (365–405 nm) to generate circular posts of photoresist after development (Microposit 351 developer, diluted 5:1 with water, Shipley Co. Inc., Marlborough, MA). The photoresist posts on the slides were heated at 120 °C for 30 min to melt the photoresist and to form lenses. After making electrical connection to the thin gold layer with silver epoxy (SPI), we electroplated ~100 nm nickel onto the exposed gold area for ~2 min at a current density of 10 mA cm<sup>-2</sup> in a warm (~45 °C) nickel sulfamate electroplating bath. A mixture of pre-polymer of PDMS and toluene (1:1 w/w) was spin-coated onto the microlens arrays at 650 rpm for 15 s and cured at 60 °C for 3 h. These photoresist lenses (index of refraction  $n_{\text{lens}} = 1.59$ ) had a thickness ~1 μm; their focal length was calculated to be ~9 μm in PDMS ( $n_{\text{PDMS}} = 1.4$ ) [18].

**Generation of Micropatterns:** An overhead projector capable of illumination at 4000 lumens (410 W/82 V, Apollo) was used as the broadband illumination source for the reduction lithography. A ground glass diffuser (1.6 mm thick, Edmund Optical) was placed in front of the bulb, inside the housing of the projector. We drew figures on CAD computer software (Macromedia Freehand 10, San Francisco, CA) and printed the cm-sized photomasks with the figures on transparency films from a desktop printer; these masks were placed on the center of the projector. Substrates for pattern formation were prepared by spinning photoresist onto Si or glass substrates. These substrates were placed in contact with the PDMS membrane covering the microlens array. The entire assembly was situated on a vertical stage ~50 cm above the transparency mask. With the lenses situated between the light source and the imaging photoresist, white light was illuminating through the mask and focused by the lenses on the photoresist. The exposed photoresist was developed in developer.

**Lift-off of Micropatterns:** The substrates for lift-off were prepared by spinning Shipley 1805 (4000 rpm for 40 s) on Si wafers. Typical exposure times were 60–90 s, and development times were between 1–2 min. After development, a Cr layer (100 nm thick) was deposited by e-beam evaporation onto the samples, and the photoresist was removed by lift-off in acetone. The Cr patterns on Si were imaged by a scanning electron microscope (LEO digital scanning electron microscope, model 982).

*Pattern Transfer with Conventional Contact Photolithography:* Silicon wafers were coated with Shipley 1805 (4000 rpm for 40 s) and were exposed through the Cr pattern for 4 s and developed for 10 s. After development, we dried the samples in a stream of nitrogen and imaged them with the scanning electron microscope.

Received: April 24, 2002  
Final version: June 5, 2002

- [1] M. H. Wu, K. E. Paul, G. M. Whitesides, *Appl. Opt.* **2002**, *41*, 2575.
- [2] H. Wu, T. W. Odom, G. M. Whitesides, *J. Am. Chem. Soc.* **2002**, *124*, 7288.
- [3] M. H. Wu, G. M. Whitesides, *J. Microelectromech. Syst.*, in press.
- [4] G. Yang, Y. Shen, *Proc. SPIE—Int. Soc. Opt. Eng.* **1998**, *3550*, 409.
- [5] M. Muellenborn, H. Dirac, J. W. Petersen, *Appl. Phys. Lett.* **1995**, *66*, 3001.
- [6] S. M. Metev, V. P. Veiko, *Laser Assisted Micro-technology*, Springer Verlag, New York **1998**.
- [7] S. Matsui, in *Handbook of Nanostructured Materials and Nanotechnologies*, Vol. 3 (Ed: H. S. Nalwa), Academic Press, San Diego, CA **2000**, p. 555.
- [8] S. Nonogaki, T. Ueno, T. Ito, “Microlithography fundamentals”, in *Semiconductor Devices and Fabrication Technology*, Marcel Dekker Inc., New York **1998**.
- [9] C. Vieu, F. Carcenac, A. Pepin, Y. Chen, M. Majias, A. Lebib, L. Manin-Ferlazzo, L. Couraud, H. Launois, *Appl. Surf. Sci.* **2000**, *164*, 111.
- [10] A. N. Broers, A. C. F. Hoole, J. M. Ryan, *Microelectron. Eng.* **1996**, *32*, 131.
- [11] J. Sone, J. Fujita, Y. Ochiai, S. Manako, S. Matsui, E. Nomura, T. Baba, H. Kawaura, T. Sakamoto, C. D. Chen, Y. Nakamura, J. S. Tsai, *Nanotechnology* **1999**, *10*, 135.
- [12] T. Deng, F. Arias, R. F. Ismagilov, P. J. A. Kenis, G. M. Whitesides, *Anal. Chem.* **1999**, *72*, 645.
- [13] T. Deng, J. Tien, B. Xu, G. M. Whitesides, *Langmuir* **1999**, *15*, 6575.
- [14] T. Deng, H. Wu, S. T. Brittain, G. M. Whitesides, *Anal. Chem.* **2000**, *72*, 3176.
- [15] D. Qin, Y. Xia, *Adv. Mater.* **1996**, *8*, 917.
- [16] J. C. Love, D. B. Wolfe, H. O. Jacobs, G. M. Whitesides, *Langmuir* **2001**, *17*, 6005.
- [17] M. H. Wu, G. M. Whitesides, *Appl. Phys. Lett.* **2001**, *78*, 2273.
- [18] H. Wu, T. W. Odom, G. M. Whitesides, *Anal. Chem.* **2002**, *74*, 3267.
- [19] G. T. A. Kovacs, *Micromachined Transducers Sourcebook*, McGraw-Hill, New York **1998**.
- [20] M. Madou, *Fundamentals of Microfabrication*, CRC Press, New York **1997**.
- [21] M. Hutley, R. Stevens, D. Daly, *Phys. World* **1991**, *4*, 27.
- [22] The edge roughness of the lines is defined as the maximal variation of the lateral dimensions of the lines.

## Hydrothermal Synthesis of Single-Crystal Ni(OH)<sub>2</sub> Nanorods in a Carbon-Coated Anodic Alumina Film\*\*

By Keitaro Matsui, Takashi Kyotani,\* and Akira Tomita

Recently, many attempts have been made to fabricate one-dimensional nanosized materials using template techniques. Several kinds of materials with straight nanochannel structures are used as templates, including anodic aluminum oxide films,<sup>[1–5]</sup> polycarbonate track-etched membranes,<sup>[6–12]</sup> nano-

\*] Prof. T. Kyotani, Dr. K. Matsui, Prof. A. Tomita  
Institute of Multidisciplinary Research for Advanced Materials  
Tohoku University, 2-1-1 Katahira, Sendai 980-8577 (Japan)  
E-mail: kyotani@tagen.tohoku.ac.jp

\*\*] We express our appreciation to the High Voltage Electron Microscope Laboratory of Tohoku University. This study was partly supported by the Tegen-Ken Project (2001) from Institute of Multidisciplinary Research for Advanced Materials, Tohoku University.